Available online at www.sciencedirect.com
SCIENCE DIRECT
Cement and Concrete Research 35 (2005) 1349–1357
Cement and Concrete Research

Influence of air-cooled slag on physicochemical properties of autoclaved aerated concrete

N.Y. Mostafa*

Chemistry Department, Faculty of Science, Suez Canal University, Ismailia 41522, Egypt

Received 9 March 2004; accepted 6 October 2004

Abstract

Lime and sand in autoclaved aerated concrete (AAC) were replaced by air-cooled slag (AS). The compressive strength and the type and nature of the hydration products were studied for samples autoclaved at 8 bar for different periods of times: 2, 6, 12 and 24 h. The hydration reactions were monitored by determining free-lime contents and combined water. The types of the hydration products were investigated using XRD and SEM/EDX. Slag substitutions for sand and lime up to 50% enhance the compressive strength, especially at short curing times (2 and 6 h). The optimum strength is obtained by 50% AS substitution for low-lime mixes (10% CaO) and 30% AS substitution for high-lime mixes (25% CaO). In high-lime mixes containing up to 30% AS, the initially formed fibrous calcium-rich CSH was changed to needle-like and lath-like 1.1 nm tobermorite. In low-lime mixes with AS-substitution, tobermorite appears at 2 h processing time with grass-like silica-rich CSH around quartz particles.

Keywords: Air-cooled slag; Hydration products; SEM; Hydrothermal; Compressive strength

1. Introduction

The most known steam cured materials are sand-lime bricks and cellular concrete or autoclaved aerated concrete (AAC). AAC is a cellular building material in which the binder consists of CSH and tobermorite. It is produced by molding and hydrothermal processing of various raw materials containing mainly quartz, Portland cement and lime with traces of aluminum powder. In the mold process, the mix slurry generates hydrogen gas by the chemical reaction between fine aluminum powder and lime.

$$2Al + 3Ca(OH)2 + 6H2O \rightarrow 3CaOAl2O3.6H2O + 3H2\uparrow$$

After the molding process, the green body is hardened by autoclaving under steam pressure, with the formation of 1.1-nm tobermorite as the main binding phase. These processes result in lightweight products with low bulk density and special desert properties, like lower thermal conductivity, lower shrinkage and higher heat resistance [1–3].

Low energy required in production, low raw material consumption, ease of use in construction and high energy efficiency add up to make AAC a very environmentally friendly building material. Nowadays, there is a worldwide enlargement in the production and usage of autoclaved aerated concrete in both hot [4,5] and cold [6,7] countries. This opened the door for replacing sand and lime (partly or wholly) by industrial waste by-products [8–11]. The advantage of this method is that it can be used to recycle materials which possess a very low reactivity at room temperature.

However, the utilization of by-products in autoclaved building materials is not only controlled by the suitability of these materials for this purpose but also by the local economy and the competitive position of other building materials within the area. Technically and economically, it may be possible to partly replace sand or lime with by-products if this is accompanied with improving the end products or reducing the production cost through reduction

* Tel.: +20 64 382216; fax: +20 64 322381.
E-mail address: nmost69@yahoo.com.

0008-8846/$ - see front matter © 2004 Elsevier Ltd. All rights reserved.
doi:10.1016/j.cemconres.2004.10.011

Table 1
Chemical composition of sand and Portland cement

	SiO_2	CaO	Al_2O_3	Fe_2O_3	MgO	MnO	Na_2O	K_2O	SO_3	L.O.I*	Total
Sand	98.2	0.3	0.43	0.34	0.2	0.15	0.02	0.05	0.01	0.5	100.2
PC	20.9	63.1	6.9	2.1	1.8	2.3	0.1	0.2	1.9	1.3	100.6

of the autoclaving time or temperature. In previous study [12], the reactivity of water-cooled (WS) and air-cooled slag (AS) produced from the same raw materials and the same blast furnace were measured at different curing conditions. Although the reactivity of AS is lower than that of WS at room temperature and 100 °C, the reactivity of AS increased much more than WS with hydrothermal activation at 180 °C. This investigation includes the study of the possibility of using the air-cooled slag by-products as substituent for sand and lime in autoclaved aerated concrete. The influences of slag substitution on the physico-mechanical and chemical properties of the final products under different autoclaving time were studied.

2. Materials

The sand was obtained from AAC Brick Company (El-Abbasah, Egypt). The chemical analysis of the sand was carried out using the XRF technique; the results of which are given in Table 1. Lime was prepared by firing analytical grade $CaCO_3$ at 1100 °C for 2 h. Each sample of lime was freshly prepared before mixing with sand to prevent or at least to minimize the contamination with atmospheric carbon dioxide. The air-cooled slag (AS) used throughout this investigation was obtained from Halwan Steel in Egypt. It is produced by slow cooling in air due to inadequate granulation facilities. Slag was ground in ball mill to attain a Blain surface area of 350 m^2/kg. The detail characterization of AS is given in another paper [13]. Portland cement was obtained from Suez Cement in Egypt. The chemical composition of Portland cement is given in Table 1, and the Blaine surface area is about 350 m^2/kg.

3. Experimental

The reference mix was taken as the mix proportion of aerated concrete produced in industry, sand 65, CaO 25 and cement 10. Slag was substituted the ingredient of AAC in

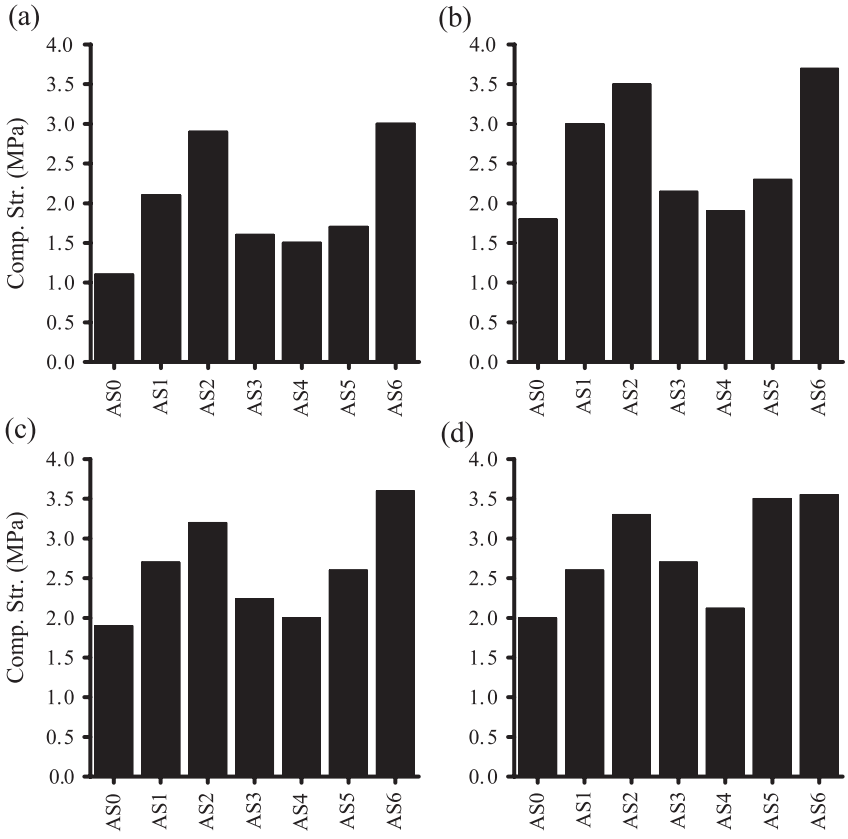

Fig. 1. Compressive strength of autoclaved aerated concrete mixes, (a) 2, (b) 6, (c) 12 and (d) 24 h.

Table 2
Autoclaved aerated concrete mixes

Mix	Mix composition			
	Sand	CaO	PC	AS
AS0	65	25	10	–
AS1	55	25	10	10
AS2	35	25	10	30
AS3	15	25	10	50
AS4	65	10	5	20
AS5	55	10	5	30
AS6	35	10	5	50

two set of mixes, high-lime mixes (25%) and low-lime mixes (10%). The predetermined proportions of sand, lime (CaO), cement and slag were weighed and thoroughly dry mixed in a ball mill. The solid mixed with water with W/S ratio of 0.7 with mechanical stirrer for 3 min, with addition of 0.05% aluminum powder. The slurries were poured into 4×4×4 cm metal mold. After several hours, the surfaces wire-cut and the cubes hydrothermally treated in an autoclave under 10 bars (183 °C) for 2, 6, 12 and 24 h. The autoclaving pressure was built up within 30 min. During cooling, the autoclave was allowed to cool down slowly until it reached the room temperature to avoid thermal and mechanical stresses within the products. After being removed from the autoclave, the samples selected for the compressive strength measurement were dried at 50 °C for 24 h. The other samples were dried at 105 °C for 24 h then subjected to physical and chemical investigations.

The physico-mechanical properties, which are considered, are strength and porosity. The kinetics of hydration of the hardened samples was followed by the determination of the chemically combined water and free lime.

X-ray diffraction (XRD) analyses were performed using an automated diffractometer (Scintag, Sunnyvale, CA) at a step size of 0.02°, scan rate of 2° per min and a scan range from 4° to 60° 2θ. Scanning electron microscopy (SEM) was performed using Hitachi S-3500N SEM instrument with variable pressure. This SEM is equipped with a secondary detector and a PGT energy dispersive X-ray analysis system. Apparent porosity was determined using the standard liquid volume method adopted by the ASTM (14).

4. Physico-mechanical properties

The porosity of all samples autoclaved for 24 h were determined according to ASTM [14]. All samples attain porosity in the range from 67% to 70% at 12 h processing time; thus, the effect of porosity on compressive strength was neglected. The changes in the compressive strengths of all the samples during 24 h autoclaving time are given in Fig. 1. The strength of the reference mix (AS0) increases during the first 6 h of autoclaving (Fig. 1, a and b). Furthermore, slow strength gain occurs at 12 and 24 h autoclaving (Fig. 1, c and d). The compressive strengths of air-cooled slag substituted samples increase more than the reference mix at all curing times. The optimum strength for mixes with low-lime contents (AS4, AS5 and AS6) is obtained by mix AS6 (50% AS), but that for mixes with higher lime contents (25% CaO) is obtained by mix AS2 (30% AS). These optimum mixes (AS2 and AS6) show a very high strength at the early curing times (2 and 6 h) than all the other mixes, followed by a small decline in strengths with further curing (see Table 2 and Fig. 1).

The large gains in the compressive strengths occur during the first 6 h for AS-substituted samples as a result of the fast lime–slag hydration reaction compared to lime–quartz reaction. Between 6 and 12 h, the strengths slightly decline for these samples then increase again at longer autoclaving times (24 h).

5. Combined water contents (Wn)

The kinetics of hydration were studied by determining the free lime contents and chemically combined water contents (Wn). At 2 h of autoclaving, the free lime of the reference mix (AS0) is 0.34% and increases to 0.53 for mix AS1. The free lime completely consumed in all other slag-containing mixes at 2 h of autoclaving. Combined water contents (Wn; Fig. 2) typically show a large increase in the first 6 h of curing for all mixes, followed by a continuous slow increase for up to 12 h. The increase in Wn is indicative of the high rate of hydration reaction at short autoclaving times, which explain the fast increase in compressive strength at these times. At 24 h of curing, the combined water contents decline for all samples. High-lime

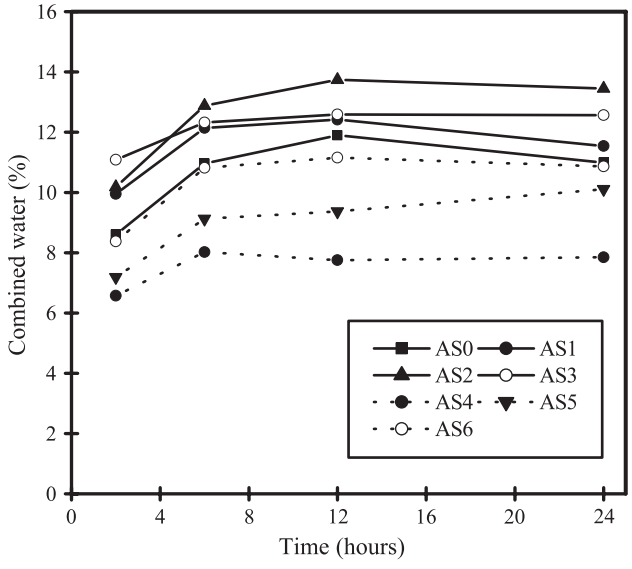

Fig. 2. Combined water contents of autoclaved aerated concrete at different curing times.

samples show larger combined water contents at all curing times than low-lime samples.

6. X-ray diffraction analysis (XRD)

X-ray diffraction analyses were carried out to identify the crystalline solid phases. The diffraction patterns are given in Figs. 3 and 4 for samples cured for 2 and 24 h, respectively. Fig. 3 shows that the peaks characteristic of tobermorite were started to appear in the reference sample (AS0) as with the low-lime samples (AS4–AS6), and the intensity increase with increasing AS contents. This indicates that tobermorite can be formed at 2 h of curing time in the presence of AS. In high-lime mixes, at this short autoclave time, the main peak of CSH intensifies with addition of AS, indicating an increase of the amount of CSH formed. No tobermorite peaks were observed at this short autoclaving time in all slag-containing samples made with 25% CaO.

The diffraction patterns of samples autoclaved for 24 h are given in Fig. 4. At this relatively long autoclaving time, 10% and 30% substitution of sand with AS intensified the characteristics tobermorite peaks (d=3.03, 11.3 and 1.83 Å) in high-lime mixes. However, 50% substitution completely retards tobermorite formation.

However, increasing the autoclaving time to 24 h in slag-containing samples made with 10% CaO has no effect on

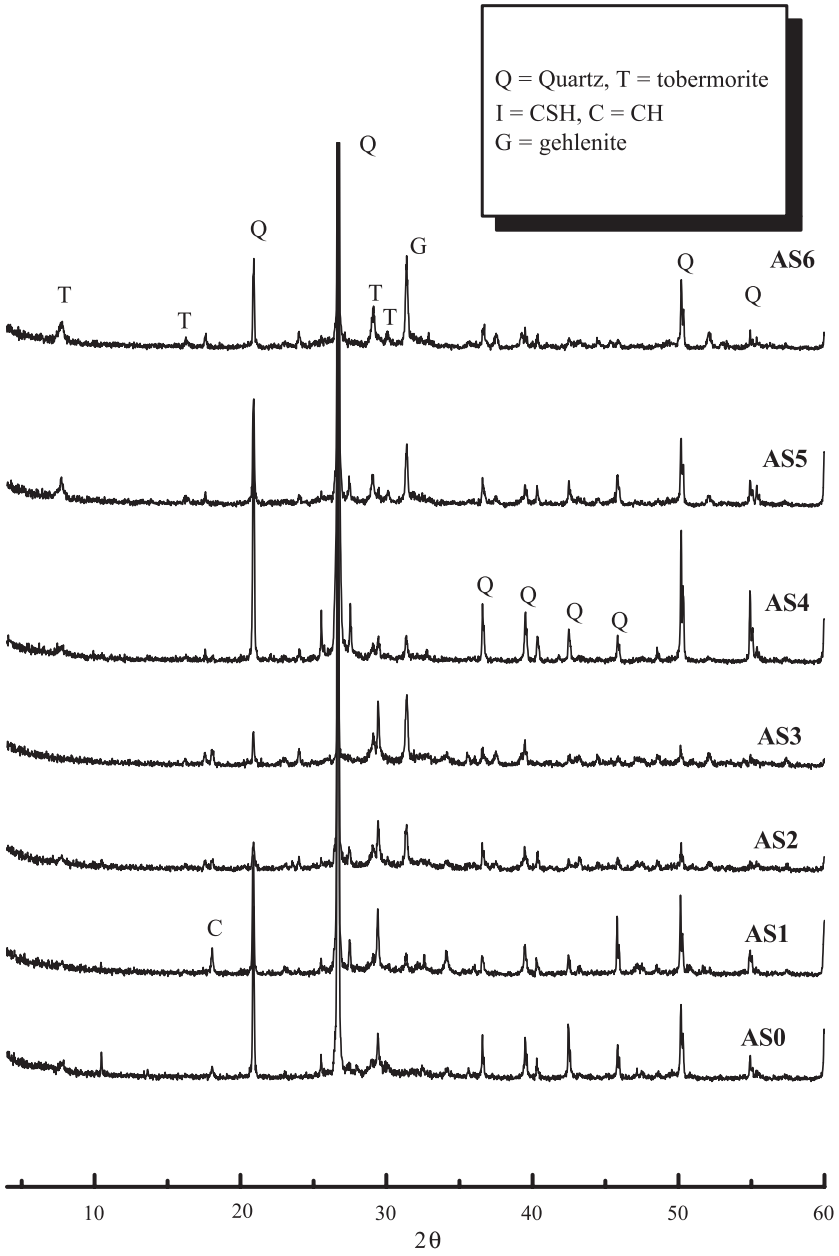

Fig. 3. XRD patterns of autoclaved aerated concrete at 2 h of curing times.

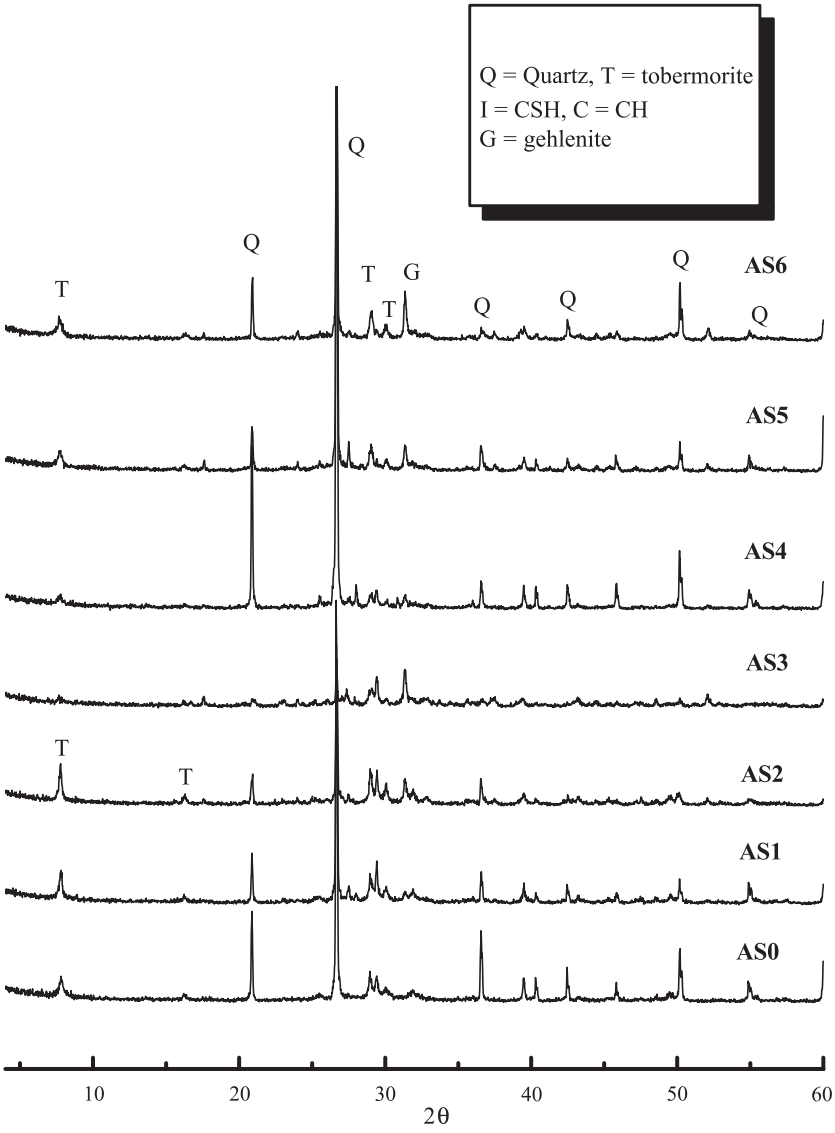

Fig. 4. XRD patterns of autoclaved aerated concrete at 24 h of curing times.

the tobermorite's peaks intensity. This indicates that tobermorite formation was inhabited after 2 h of autoclaving in these mixes.

7. Electron microscopy (SEM)

The fracture surface of all samples autoclaved for 2 and 24 h are examined with scanning electron microscopy. Fig. 5a and b shows the change in microstructure in the reference mix (AS0). The initially formed amorphous CSH and platy-like tobermorite (Fig. 5a) change to crumbled foiled tobermorite (Fig. 5b) with further processing.

In high-lime mixes made with 10 and 30% AS substitution (AS1 and AS2), at 2-h processing time, only fibers CSH are formed. At 24-h processing time, these CSH fibers change to a very crystalline needle-like tobermorite. Fig. 6 is given as example of this change for sample AS2.

Fig. 7 shows no tobermorite formed in mix AS3 (50% AS substitution) at all autoclaving times. Rather, amorphous Al-substituted CSH formed (Fig. 7a), and it changed to reticulated amorphous CSH (Fig. 7b) with increasing processing time. This seems to be due to the increase in the bulk C/S ratio beyond those suitable for tobermorite formation.

In AS-substituted mixes made with low-CaO contents (10%), tobermorite appears at 2-h processing time. However, with further processing, tobermorite formation was retarded and CSH with a grass-like structure, and a very low C/S ratio was formed. Figs. 8 and 9 are the SEM picture for mix AS5 and AS6, respectively.

8. Discussion

Introducing slag in to such high silica $CaO–SiO_2–H_2O$ system has two effects. The first one is the difference in

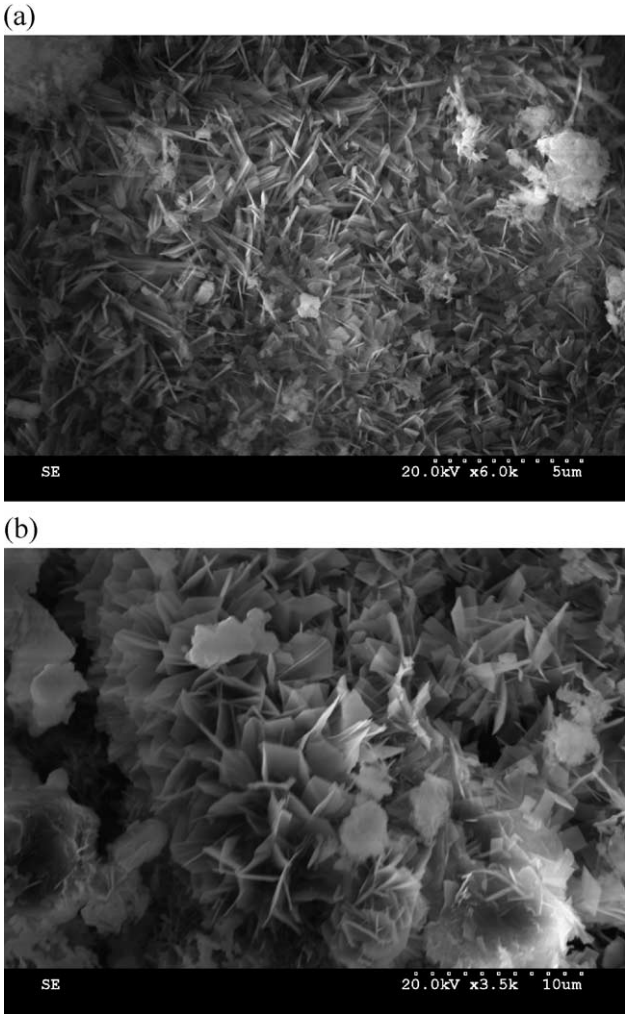

Fig. 5. SEM micrographs of the reference mix (AS0) at (a) 2 and (b) 24 h.

reactivity between quartz and slag. Air-cooled slag has higher reactivity than quartz, and the reactivity increases with temperature [12]. Slag-substituted samples consume the lime faster than slag-free samples, and thus, also, the also combined water increases as a result of the increasing amount of calcium silicate hydrate formed. This effect is the main factor in increasing the compressive strengths of slag-substituted samples at short autoclaving time (2 h). This suggests that the utilization of slag have an advantage of reducing the curing time or reducing the curing temperature in the autoclave. The former advantage is very important in increasing the plant output to satisfy the market needs, and the later advantage is very critical in old autoclaving chambers which cannot hold a very high pressure.

The second effect of introducing slag is the modification of the equilibrium in the $CaO–SiO_2–H_2O$ system. The high reactivity of the added slag modifies this system by introducing Al and increases the Ca/Si ratio. These two modifications have opposite effects on the rate of tobermorite formation, which is the main binding phase in autoclaved Ca-silicate building products. In this investigation, the substitution of slag up to 50% with about 10–11% Al_2O_3 does not result in the formation of new Al-containing phases, such as hydrogarnetes. It seems that all the aluminum can be accommodated in either the CSH-gel or the tobermorite. The effect of Al substitution on the stability field and rate of crystallization of tobermorite have been studied by many investigators [15–18]. They showed that the presence of Al^{3+} accelerates the rate of tobermorite crystallization. Isu et al. [19] find that addition of slag to autoclaved aerated concrete gives tobermorite with high Al substitution and lower Ca/(Al+Si) ratio than samples without slag, and also, the crystallinity increases. The author reported [20] that the presence of Al-ions could lower the temperature required for the formation of tobermorite down to 100 °C at 14 days of autoclaving times. In the present study, up to 50% substitution of sand by slag accelerates the tobermorite formation at 2 h in low-lime mixes (10% CaO). In these mixes, the formation of tobermorite from CSH is accelerated due to the presence of aluminum ion and

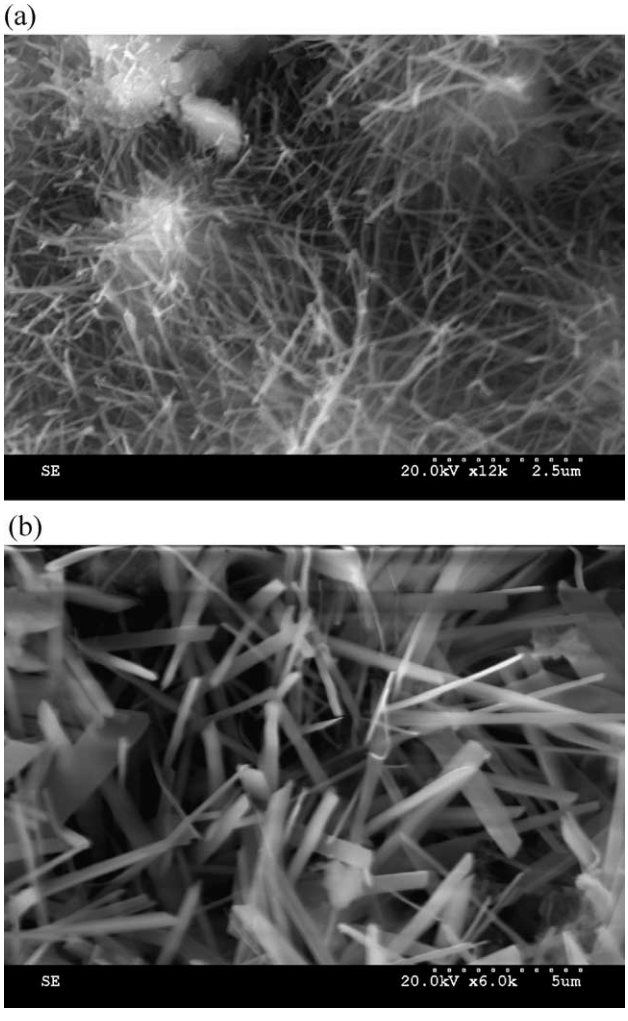

Fig. 6. SEM micrographs of mix (AS2) at (a) 2 and (b) 24 h.

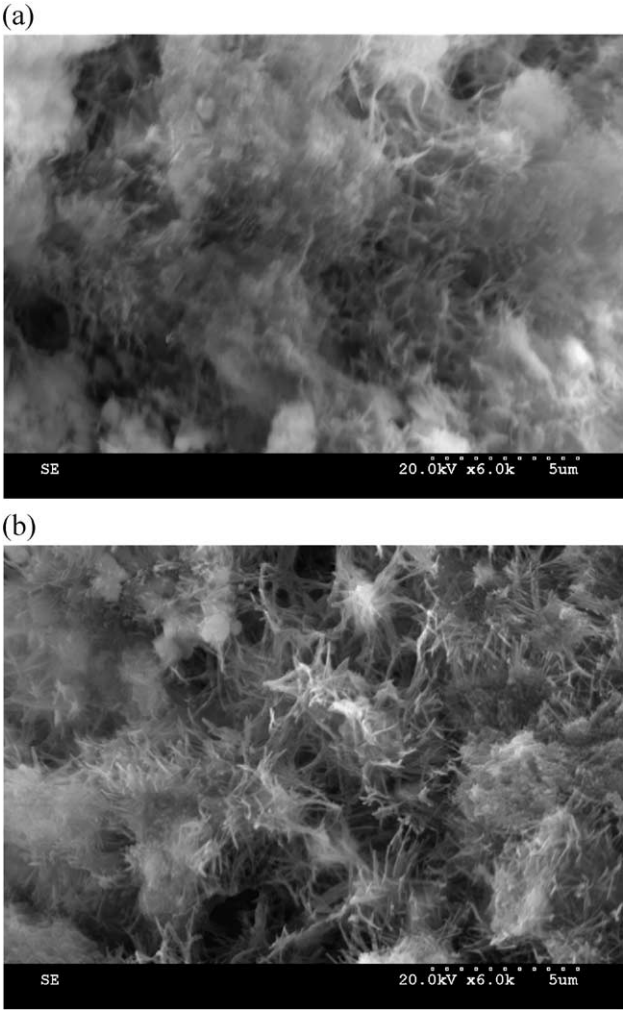

Fig. 7. SEM micrographs of mix (AS3) at (a) 2 and (b) 24 h.

suitable available C/S ratio for tobermorite formation. As the lime consumed, with longer autoclaving times, the available C/S ratio becomes lower than the limit under which further formation of tobermorite is inhibited. Since at very low C/S ratio, tobermorite can not formed even with presence of some accelerator like Al and sulfate ions and long autoclaving times [20–22]. Okada et al. [23] noted the C/S ratio of the initially formed CSH-gel controls the rate of its transformation to tobermorite. In CaO and quartz mixtures (Ca/Si=0.8), the initial C–S–H with a Ca/Si of 1.69 transformed to tobermorite having a C/S<0.9. In a comparison sample made with silicic acid and CaO (C/S=0.8), the initial C–S–H had a Ca/Si=0.81, and tobermorite crystallization was significantly slower. Okada's results [23] were confirmed by Sato and Grutzeck [24] using ^{29}Si NMR to study samples prepared from CaO and quartz, silicic acid or colloidal silica fume at 180 °C. The C–S–H which formed initially in the quartz samples was characterized by a low Q_2/Q_1 ratio (i.e., short chains, dimers) and tobermorite crystallized by 4 h. In samples made from silicic acid and silica fume, the initial C–S–H had a high Q_2/Q_1 plus Q_3 (i.e., long chains, some cross-linking). Even after 24 h, these samples did not convert to crystalline tobermorite. Tobermorite formed easily from the C–S–H with high C/S ratio but not from the Si-rich ones, which indicates that the C–S–H gel structure affects the ease of tobermorite crystallization. The presence of long, cross-linked chains in the Si-rich C–S–H retards the rearrangement of silica tetrahedra that is needed to form tobermorite. On the other hand, the short chains and dimers in the Ca-rich C–S–H can rearrange more easily to form crystalline tobermorite. In the present study, the low C/S ratio promotes the formation of poorly crystalline CSH and prevents the tobermorite formation at long autoclaving times.

In high-lime mixes, addition of slag up to 30% increases tobermorite crystallinity at long autoclaving times. However, 50% slag prevents the formation of tobermorite due to the increase in the available Ca/Si ratio beyond the Ca/Si ratio suitable for its formation. Thus, Ca-rich CSH is formed at short autoclaving time (2 h). This

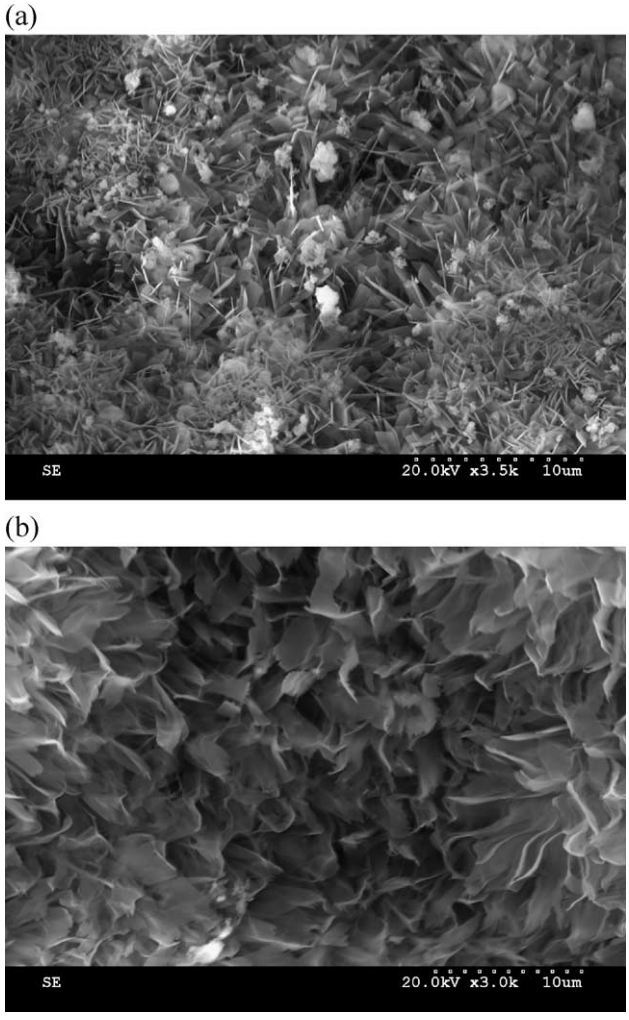

Fig. 8. SEM micrographs of mix (AS5) at (a) 2 and (b) 24 h.

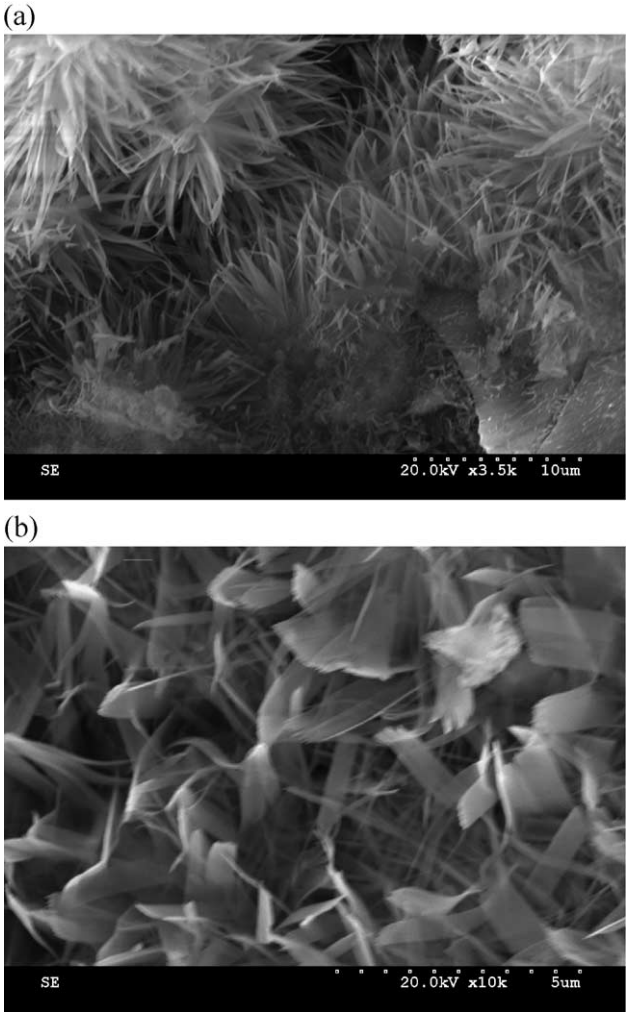

Fig. 9. SEM micrographs of mix (AS6) at (a) 2 and (b) 24 h.

Ca-rich CSH transform to a crystalline tobermorite at longer autoclaving times.

9. Conclusions

The present study has shown that air-cooled slag can be used as a valuable additive to autoclaved aerated concrete. The substitution of sand with AS in autoclaved building materials accelerate the tobermorite formation if the reactive C/S ratio was adjusted. This may used to reoptimize the production cost to lower autoclaving time, which is an economical option for developing countries. This will be associated with advantages in the production of AAC:

(1) increasing the plant output;
(2) decreasing the production cost through the reduction of the autoclaving conditions and the reduction in the amount of lime used; and
(3) improving the end products of AAC with respect to the mechanical properties.

A possible disadvantage of AS substitution is the dark color of the end products at the higher substitution level.

Acknowledgements

The author wishes to thank Prof. Paul W. Brown, The Pennsylvania State University, for the help and useful discussion.

References

[1] S. Aroni, On energy conservation characteristics of autoclaved aerated concrete, Mat. Struct. 23 (133) (1990) 68–77.
[2] A. Nielsen, Shrinkage and creep deformation parameters of aerated autoclaved concrete, Preprints-RILEM International Symposium on Autoclaved Aerated Concrete. Organ at Swiss Fed. Inst. of Technol. Sponsored by: RILEM, Paris, 1982, pp. 175–191.
[3] R. Lawrence, D.N. Ronald, Thermal inertia properties of autoclaved aerated concrete, J. Energy Eng. 125 (2) (1999) 59–75.
[4] H.A. Al-Mudhaf, E.K. Attiogbe, Performance of autoclaved aerated-concrete masonry walls in Kuwait, Mater. Struct./Mater. Constr. 29 (1996) 448–452.
[5] M.H. Wajahat, A.I. Soliman, Utilisation of Saudi sands for aerated concrete production, Int. J. Cem. Compos. Lightweight Concr. 8 (2) (1986) 81–85.
[6] E. Ian, Aircrete blockwork, Concrete (Lond.) 31 (7) (1997) 10–11.
[7] Y. Houst, and F.H. Wittmann, Bibliography on autoclaved aerated concrete, Developments in Civil Engineering, Sponsored by: RILEM, Paris, Fr. Elsevier Scientific Publ. Co., 1983, pp. 325–369.
[8] H. Andre, E. Urs, M. Thomas, Fly ash from cellulose industry as secondary raw material in autoclaved aerated concrete, Cem. Concr. Res. 29 (3) (1999) 297–302.
[9] D. Briesemann, Structural elements and masonry of autoclaved aerated concrete, Preprints-RILEM International Symposium on Autoclaved Aerated Concrete. Organ at Swiss Fed. Inst. of Technol., Sponsored by: RILEM, Paris, 1982 pp. 241–249.
[10] K.C. Verma, Scenario of utilization of fly ash in India, Irrig. Power J. 51 (2) (1994) 69–74.
[11] S.A.S. El-Hemaly, A.S. Taha, H. El-Didamony, Influence of slag substitution on some properties of sand–lime aerated concrete, J. Mater. Sci. 21 (4) (1986) 1293–1296.
[12] N.Y. Mostafa, S.A.S. El-Hemaly, E.I. Al-Wakeel, S.A. El-Korashy, P.W. Brown, Hydraulic activity of water-cooled slag and air-cooled slag at different temperatures, Cem. Concr. Res. 31 (2001) 475–484.
[13] N.Y. Mostafa, S.A.S. El-Hemaly, E.I. Al-Wakeel, S.A. El-Korashy, P.W. Brown, Characterization and evaluation of the hydraulic activity of water-cooled slag and air-cooled slag, Cem. Concr. Res. 31 (2001) 899–904.
[14] ASTM C 373–88, Water absorption, bulk density, apparent porosity and apparent specific gravity of fired whiteware products, (1999).
[15] S.A.S. El-Hemaly, T. Mitsuda, H.F.W. Taylor, Synthesis of normal and anomalous tobermorites, Cem. Concr. Res. 7 (1977) 429–438.
[16] R. Gabrovsek, B. Kurbus, Z. Lengar, Comparison of unsubstituted and aluminum containing synthetic tobermorite characterized by different methods, Cem. Concr. Res. 16 (1986) 325–332.
[17] M. Sakiyama, T. Mitsuda, Hydrothermal reaction between C–S–H and kaolinite for the formation of tobermorite at 180 °C, Cem. Concr. Res. 7 (1977) 681–686.
[18] M.W. Barnes, B.E. Scheetz, The chemistry of Al-tobermorite and its coexisting phases at 175 °C, in: B.E. Scheetz, A.G. Landers, I. Older, H. Jennings (Eds.), Special Cements with Advanced Properties, vol. 179, Mater. Res. Soc. Symp. Proc., Boston, MA, Mat. Res. Soc, Pittsburgh, PA, 1991, pp. 243–272.

[19] N. Isu, K. Sasaki, H. Ishida, T. Mitsuda, Mechanical property evolution during autoclaving process of aerated concrete using slag: I. Tobermorite formation and reaction behavior of slag, J. Am. Ceram. Soc. 77 (8) (1994) 2088–2092.
[20] N.Y. Mostafa, S.A.S. El-Hemaly, E.I. Al-Wakeel, S.A. El-Korashy, P.W. Brown, Activity of silica fume and dealuminated kaolin at different temperatures, Cem. Concr. Res. 31 (2001) 905–911.
[21] Z. Sauman, Influence of SO_4^{2-} ions on the formation of 11A°-tobermorite, 3rd Inter. Symp. Auto. Calc. Silic. Chem., Brno, vol. 25, 1972, pp. 31–35.
[22] N.Y. Mostafa, Factors effecting the hydrothermal reactions in CaO–SiO_2–H_2O system, MS thesis, Suez Canal university, December (1995).
[23] Y. Okada, M. Shimoda, T. Mitsuda, and H. Toraya, Synthesis of tobermorite: NMR spectroscopy and analytical electron microscopy, Onoda Company Report, vol. 42, part 2, (1990) pp.123–131.
[24] H. Sato, M.W. Grutzeck, Effect of starting materials on the synthesis of tobermorite, Proc. Mater. Res. Soc. Symp., Boston, MA, 1991, pp. 235–240.